TECHNICAL NOTES

NATIONAL ADVISORY COMMITTEE FOR AERONAUTICS

No. 784

# STRESS DISTRIBUTION IN AND EQUIVALENT WIDTH OF FLANGES OF WIDE, THIN-WALL STEEL BEAMS

By George Winter
Cornell University



Washington
November 1940

NATIONAL ADVISORY COMMITTEE FOR AERONAUTICS

TECHNICAL NOTE NO. 784

# STRESS DISTRIBUTION IN AND EQUIVALENT WIDTH OF FLANGES OF WIDE, THIN-WALL STEEL BEAMS*

By George Winter

## SUMMARY

The use of different forms of wide-flange, thin-wall steel beams is becoming increasingly widespread. Part of the information necessary for a rational design of such members is the knowledge of the stress distribution in and the equivalent width of the flanges of such beams. This problem is analyzed in this paper on the basis of the theory of plane stress. As a result, tables and curves are given from which the equivalent width of any given beam can be read directly for use in practical design. An investigation is given of the limitations of this analysis due to the fact that extremely wide and thin flanges tend to curve out of their plane toward the neutral axis. A summary of test data confirms very satisfactorily the analytical results.

## INTRODUCTION

This paper deals with the distribution of longitudinal stresses in the flanges of thin-wall beams of I-, T-, or box shape, or of similar shape.

Beams such as I- and other rolled sections and composites thereof have long been in use in structural engineering, and it is generally assumed that the magnitude of the longitudinal stresses does not vary over the width

---

*Condensed from a thesis accepted by the Graduate School of Cornell University in partial fulfillment for the degree of Doctor of Philosophy, June 1940.

This analysis was undertaken in parallel with an experimental investigation into this subject sponsored by the American Iron and Steel Institute at Cornell University.

of the flange at a given cross section. With the development of light-weight constructions of different kinds there is, however, at present a definite trend toward the use of I-, T-, and other sections of considerable width and rather small thickness. Structural members of such kind are widespread in ship and airplane building and, with the development of the spot-welding technique, are becoming increasingly important for small-scale structures such as residence buildings. In connection with this development, investigations have been undertaken to ascertain whether in such cases the bending stresses still may be assumed to be uniformly distributed over the width of the flange. (See references 1, 2, and 3.) It was found that in wide beams the stress distribution considerably deviates from uniformity and that for a rational design of such beams this nonuniformity must be taken into account. All these investigations which treat the behavior of the beam as a whole are concerned with special cases. Moreover, very complex mathematical expressions are arrived at which, for numerical evaluation, require an amount of algebraic computation prohibitive in design practice. In addition, the stress distribution in the flanges is treated as a problem in plane stress without analyzing the limitations arising from this approach.

The present work, in which a different method was used, undertakes to investigate the stress distribution in the flanges of I-, T-, U-, and box-shape beams and to present the numerical results in the form of tables and curves for direct use in practical design work. In order to achieve this purpose, two steps are necessary: (1) The state of stress in the flanges is analyzed for different loading conditions and as a result curves are presented from which the equivalent width for practically all possible beam dimensions can be read directly; and (2) an investigation is carried out to ascertain the limits within which this analysis, based on plane stress, is sufficiently exact; as a result, simple formulas are given for the limiting dimensions of beams to which the foregoing analysis applies. In addition, it seemed desirable to provide possibilities for experimental verification of this analysis. For this purpose, a further curve is computed, which gives the ratio of the magnitudes of the stresses at the center of the flange to that at the edges for I-beams. These ratios can be checked experimentally by strain measurements.

## THEORETICAL ANALYSIS OF STRESS DISTRIBUTION

### General Method

For practical design work it is important to ascertain that the actual stresses at no point exceed a given limiting working stress. In order to achieve this objective, it is simplest to make use of the idea of the equivalent width. In figure 1 the actual stress distribution over the width of the flange of an I-beam is given in full lines. The area under this curve, multiplied by the flange thickness, represents the total longitudinal force acting in the flange. If this area is replaced by a rectangle (dotted lines on fig. 1) of equal magnitude, the depth of which is equal to the actual maximum stress $\sigma_{max}$, an equivalent width $2b'$ is obtained. Obviously the flange of width $2b$ with its actually nonuniform stress distribution may then, for all practical purposes, be replaced by a fictitious flange of the same thickness, but of equivalent width $2b'$ and of uniform stress distribution. In particular, the section modulus will then be computed on the basis of $2b'$ instead of $2b$, and as a result the stress found from the elementary formula $\sigma_{max} = M/S$ will then coincide with the actual $\sigma_{max}$ in the flange.

Throughout this investigation the x-axis of the coordinate system is taken in the longitudinal direction of the beam, and the y-axis is taken as shown in figure 1, and the z-axis is taken in the vertical direction. If $d$ is the thickness of the flange, the total longitudinal force acting in the flange becomes

$$F = 2d \int_0^b \sigma_x \, dy \qquad (1)$$

and the equivalent width is obtained from

$$2b' = \frac{F}{d\,\sigma_{max}} = \frac{2}{\sigma_{max}} \int_0^b \sigma_x \, dy \qquad (2)$$

If, for the moment, the small curvature of the beam due to bending is neglected, the flange may be regarded as a plane plate loaded by shearing forces along its joint

with the web. It is then possible to investigate the resulting stress distribution by means of the theory of plane stress. The distribution of the shear stresses along the joint of web and flange evidently follows the distribution of the external shearing force in the beam as a whole. This assumption holds exactly only for beams loaded by continuously distributed loads. Concentrated loads result in local irregularities of the shear distribution because of the distributing action of the web and because of the actual area of application of such so-called concentrated loads. The influence of these factors will be investigated later in this paper. Thus the total shear T transmitted from the web to the flange at any particular cross section is proportional to the external shearing force V, namely,

$$T = \frac{n}{I} V = k V \tag{3}$$

where n is moment of area of flange about neutral axis and I is moment of inertia of the beam. The stress distribution of a plane plate loaded in that manner will now be analyzed.

Throughout this investigation the span of the beam is taken as 2l and the width of the flange as 2b; the thickness of the flange is taken as unity. Thus figure 2(a) represents the flange of an I-beam loaded by a single concentrated force in the center; figure 2(b) shows the flange of a box beam under uniform load. Because the problem is one in plane stress, the solution reduces to the integration of the differential equation. (See reference 4.)

$$\frac{\partial^4 \phi}{\partial x^4} + 2 \frac{\partial^4 \phi}{\partial x^2 \partial y^2} + \frac{\partial^4 \phi}{\partial y^4} = 0 \tag{4}$$

where $\phi$ is the Airy stress function. Then the stresses are

$$\sigma_x = \frac{\partial^2 \phi}{\partial y^2} \tag{5a}$$

$$\sigma_y = \frac{\partial^2 \phi}{\partial x^2} \tag{5b}$$

$$\tau_{xy} = - \frac{\partial^2 \phi}{\partial x \partial y} \tag{5c}$$

where $\sigma_x$ is the longitudinal stress; $\sigma_y$, the transverse stress; $\tau_{xy}$, the horizontal shear stress. Equation (4) is satisfied by any function of the form

$$\phi = \sum_{1}^{n} (A_n \cosh \alpha_n y + B_n \sinh \alpha_n y + C_n y \cosh \alpha_n y + D_n y \sinh \alpha_n y) \cos \alpha_n x \quad (6)$$

where

$$\alpha_n = \frac{n\pi}{2l}$$

The constants $A_n$, $B_n$, $C_n$, $D_n$ follow from the boundary conditions. By substitution of $\phi$ (equation (6)) in equation (5c) it is possible to represent the distribution of $\tau_{xy}$ along the loaded edge of the plate as a Fourier series. The boundary conditions common to both types of beams (see figs. 2(a) and 2(b)) are:

$$\sigma_y = 0 \text{ at } y = \pm b$$

and

$$\sigma_x = 0 \text{ at } x = \pm l$$

The second of these conditions is satisfied by making n odd. Two constants are required to satisfy the first condition. In addition, there are two more conditions in $\tau_{xy}$ along the longitudinal edges that vary according to the particular case. Thus, two more constants are required to satisfy these conditions, and hence all four constants are determined. It may be noted that this solution results in a set of horizontal shearing stresses along the short edges $x = \pm l$, which may or may not coincide with the actual distribution in any given beam, depending on the type of practical end support. However, because of equilibrium and symmetry, the resultant of these stresses is zero along either edge. Therefore, these stresses, according to Saint-Venant's principle, have only local effects, which disappear at a short distance from the edge. But from the designer's point of view only the stress distribution at and near the cross section of maximum moment, that is, near the center portion of the beam, is of interest. These stresses will not be affected by the shearing stresses along $x = \pm l$.

Having thus determined all four constants, one is able to compute the stresses at any point of the flange by means of equation (5) and the equivalent width from equation (2).

## Stress Distribution in I- and T-Beams

The general solution just outlined applies only to plates loaded along their edges. Since, for I- and T-beams, the shear from the web acts along the center line of the flange, let the flange be cut in half along the x-axis. The distribution of these applied shear stresses at $y = 0$ is expanded in a Fourier series in sine only and with $n$ odd. Let $K_n$ be the coefficients of this series. Then the boundary conditions are:

(1) At $y = 0$, $\tau_{xy} = \sum_{1}^{n} K_n \sin \alpha_n x$

(2) At $y = b$, $\sigma_x = 0$

(3) At $y = b$, $\tau_{xy} = 0$

(4) Since the plate is cut in half along the x-axis, there is the further condition that the two halves are prevented from separating along the cut. Since bodily translation or rotation of either half is prevented by equilibrium and symmetry, this condition results at $y = 0$ in $\frac{\partial^2 v}{\partial x^2} = 0$.

Conditions (1), (2), and (3) are evaluated by using for $\sigma_x$ equation (5a), for $\tau_{xy}$ equation (5c), and for $\phi$ equation (6). In order to evaluate condition (4), let $u$ be the displacement in the x-direction and $v$ in the y-direction. Then the longitudinal strain

$$\epsilon_x = \frac{\partial u}{\partial x} = \frac{1}{E} (\sigma_x - \nu \sigma_y) = \frac{1}{E}\left( \frac{\partial^2 \phi}{\partial y^2} - \nu \frac{\partial^2 \phi}{\partial x^2} \right) \qquad (7a)$$

and the shear strain

$$\gamma_{xy} = \frac{\partial u}{\partial y} + \frac{\partial v}{\partial x} = \frac{1}{G} \tau_{xy} = -\frac{1}{G} \frac{\partial^2 \phi}{\partial x \partial y} \qquad (7b)$$

where $E$ is Young's modulus, $\nu$ is Poisson's ratio, and $G=\frac{E}{2(1+\nu)}$ is the modulus of elasticity in shear. If equation (7a) is differentiated with respect to $y$

$$\frac{\partial^2 u}{\partial x \partial y} = \frac{1}{E}\left(\frac{\partial^3 \phi}{\partial y^3} - \nu \frac{\partial^3 \phi}{\partial x^2 \partial y}\right) \tag{8a}$$

And if equation (7b) is differentiated with respect to $x$, with $\left(\frac{\partial^2 v}{\partial x^2}\right)_{y=0} = 0$

$$\left(\frac{\partial^2 u}{\partial x \partial y}\right)_{y=0} = -\frac{1}{G}\left(\frac{\partial^3 \phi}{\partial x^2 \partial y}\right)_{y=0} \tag{8b}$$

If the right sides of equations (8a) and (8b) are equated, it is seen that at $y = 0$

$$-\frac{1}{G}\left(\frac{\partial^3 \phi}{\partial x^2 \partial y}\right)_{y=0} = \frac{1}{E}\left(\frac{\partial^3 \phi}{\partial y^3} - \nu \frac{\partial^3 \phi}{\partial x^2 \partial y}\right)_{y=0} \tag{8c}$$

Equation (8c) and conditions (1), (2), (3), result in four simultaneous equations in $A_n$, $B_n$, $C_n$, $D_n$. Solving these, the four constants are

$$A_n = -K_n \frac{(1-\nu)\sinh^2 \alpha_n b + (1+\nu)(\alpha_n b)^2}{\alpha_n^2(\sinh 2\alpha_n b + 2\alpha_n b)} \tag{9a}$$

$$B_n = K_n \frac{1-\nu}{2\alpha_n^2} \tag{9b}$$

$$C_n = K_n \frac{1+\nu}{2\alpha_n} \tag{9c}$$

$$D_n = -K_n \frac{(1+\nu)\cosh^2 \alpha_n b + (1-\nu)}{\alpha_n(\sinh 2\alpha_n b + 2\alpha_n b)} \tag{9d}$$

All these constants are expressed in $K_n$, that is, in terms of the Fourier coefficients of the shear distribution series along the loaded edges. It is therefore possible to adapt the solution to any given type of loading.

## Stress Distribution in Box and U-Beams

The flanges of such beams are loaded by shearing stresses along both longitudinal edges. (See fig. 2(b)). The distribution of these stresses again is expanded in a Fourier series in sine only and with n odd, the coefficients of which are $K_n$. Then the boundary conditions are:

(1) At $y = \pm b$, $\tau_{xy} = \pm \sum_{1}^{n} K_n \sin \alpha_n x$

(2) At $y = \pm b$, $\sigma_y = 0$

(3) And by symmetry, at $y = 0$, $\tau_{xy} = 0$

If equations (5a), (5c), and (6) are used, four simultaneous equations are again arrived at from which

$$A_n = -K_n \frac{2 b \sinh \alpha_n b}{\alpha_n(\sinh 2 \alpha_n b + 2 \alpha_n b)} \tag{10a}$$

$$B_n = 0 \tag{10b}$$

$$C_n = 0 \tag{10c}$$

$$D_n = K_n \frac{2 \cosh \alpha_n b}{\alpha_n(\sinh 2 \alpha_n b + 2 \alpha_n b)} \tag{10d}$$

## Equivalent Width for Different Loading Conditions

In order to derive data for use in practical design, three kinds of loading are investigated for both types of beams and for different ratios of width to span, b/l. The types of loading and the corresponding shear distributions are shown in figure 3. These shear distributions are expanded in Fourier series in sine only and with n odd. The respective Fourier coefficients are:

For loading (a)

$$K_n = \pm \frac{1}{n^2} \tag{11a}$$

For loading (b),

$$K_n = \frac{1}{n} \tag{11b}$$

For loading (c),

$$K_n = \pm \frac{1}{n} \sin \frac{n\pi}{4} \tag{11c}$$

If these coefficients are introduced into equations (9) and (10), the stress function $\phi$ is then determined from equation (6).

In order to compute the equivalent width $2b'$, use is made of equation (2). Introducing into this equation $\sigma_x$ from equation (5a)

$$2b' = \frac{2\int_0^b \sigma_x dy}{\sigma_{max}} = \frac{2\int_0^b \frac{\partial^2 \phi}{\partial y^2} dy}{\sigma_{max}} = \frac{2 \left.\frac{\partial \phi}{\partial y}\right|_{y=0}^{y=b}}{\sigma_{max}} \tag{12}$$

The maximum stress $\sigma_{max}$ (see fig. 1) occurs at the web, that is, at $y = 0$ in I-beams and at $y = \pm b$ in box beams. Thus,

$$\sigma_{max} = \left(\frac{\partial^2 \phi}{\partial y^2}\right)_{y=0} \quad \text{for I-beams, and}$$

$$\sigma_{max} = \left(\frac{\partial^2 \phi}{\partial y^2}\right)_{y=b} \quad \text{for box beams}$$

For design purpose it is the ratio of the equivalent to the actual width $2b'/2b$ that is important. If $\sigma_{max}$ is substituted into equation (12), one obtains for I-beams

$$\frac{2b'}{2b} = \frac{1}{b} \frac{\left.\frac{\partial \phi}{\partial y}\right|_{y=0}^{y=b}}{\left(\frac{\partial^2 \phi}{\partial y^2}\right)_{y=0}} \tag{13a}$$

and for box beams

$$\frac{2b'}{2b} = \frac{1}{b} \frac{\left.\frac{\partial \phi}{\partial y}\right|_{y=b}}{\left(\frac{\partial^2 \phi}{\partial y^2}\right)_{y=b}} \qquad (13b)$$

Having obtained the reduction factor $2b'/2b$, it is then possible to determine the equivalent width of any given beam, multiplying the actual width by the appropriate reduction factor. The maximum stress is then obtained from the ordinary flexure formula

$$\sigma_{max} = \frac{M}{S'}$$

where $M$ is the bending moment and $S'$ is the reduced section modulus determined by using the equivalent width $2b'$ instead of the actual width $2b$.

The stress concentration and hence the equivalent width vary along the beam. For concentrated loads the concentration is largest, that is, the equivalent width is the smallest, at the point where load is applied, which usually is also the section of maximum moment. For beams with uniformly distributed load, the maximun moment acts at the center of the span, and hence it is this place for which the reduction factor is to be determined. For use in design, reduction factors pertaining to the sections just mentioned have been computed for a wide range of span:width. It is easily seen that the reduction factors for loadings (b) and (c) of figure 3 are identical. A comparison of equations (11b) and (11c) reveals that $K_n$ for loading (c) is obtained from $K_n$ for loading (b) through multiplication by $\begin{matrix} +- \\ -+ \end{matrix} \frac{1}{\sqrt{2}}$. For loading (b), however, the critical cross section is the center of the span where $\cos \alpha_n x = \cos 0 = 1$; whereas for loading (c) it is the quarter points where $\cos \alpha_n x = \cos \frac{n\pi}{4} = \begin{matrix} +- \\ -+ \end{matrix} \frac{1}{\sqrt{2}}$. Hence, the stresses at that point are obtained from those at the center for loading (b) by multiplying the series for $\sigma_x$, term by term, by 1/2. Since this factor appears both in the numerator and in the denominator of the reduction factor $2b'/2b$ (see equation (12)), the equivalent widths for both types of concentrated loads are identical.

It is therefore safe to apply this reduction factor to any type of concentrated loading.

In table I numerical data are given for the reduction factors of both types of beams investigated and for distributed and concentrated loading.

TABLE I

Ratios of Equivalent to Actual Width, $2b'/2b$

| Beams | I- and T- | | Box and U- | |
|---|---|---|---|---|
| l/b | $p^{(a)}$ | $P^{(b)}$ | $p^{(a)}$ | $P^{(b)}$ |
| $\pi$ | 0.657 | 0.575 | 0.880 | 0.557 |
| $2\pi$ | .958 | .791 | .957 | .778 |
| $3\pi$ | .981 | .881 | .983 | .881 |
| $4\pi$ | .990 | .927 | .989 | .926 |
| $5\pi$ | .993 | .949 | .994 | .950 |

$^{(a)}p$ is uniformly distributed load

$^{(b)}P$ is concentrated load at center of span or two equal concentrated loads at quarter points.

The only numerical results given in Schnadel's paper on box beams (reference 2) pertain to a beam of ratio span : width = $\pi$. For this beam Schnadel found for $2b'/2b$ the following values: 0.553 for center load, 0.382 for uniformly distributed load, and 0.547 for quarter-point loads. It is seen that the differences between the results obtained by Schnadel's cumbersome method and those obtained by present simple approach are negligible for all practical purposes.

It follows from table I that the reduction factors for I- and T-beams are practically identical with those for box and U-beams except for extremely wide beams. For design work the values for I- and T-beams may therefore be

used also for box and U-beams. For more convenient use these factors are presented in figure 4 in the form of two curves from which for any particular beam and loading the reduction factor can be read immediately.

## EXPERIMENTAL VERIFICATION

In order to facilitate an experimental test of these analytical results, it seems desirable to develop data that can be directly measured on test specimens. For this reason the ratios $\sigma_{max}/\sigma_{min}$ have been computed for I-beams, where

$$\sigma_{max} = \left(\frac{\partial^2 \phi}{\partial y^2}\right)_{y=o} \quad \text{and} \quad \sigma_{min} = \left(\frac{\partial^2 \phi}{\partial x^2}\right)_{x=b}$$

The results are given in table II.

TABLE II

Ratios of Maximum Stress at Web to Minimum Stress at Edge of Flange for I-beams, $\sigma_{max}/\sigma_{min}$

| l/b | p | P |
|---|---|---|
| $\pi$ | 1.30 | 2.50 |
| $2\pi$ | 1.07 | 1.46 |
| $3\pi$ | 1.03 | 1.23 |
| $4\pi$ | 1.015 | 1.14 |
| $5\pi$ | 1.005 | 1.09 |

Extensive experimental work has been carried out to check the analytical results. It included wide-flange rolled sections (d = 0.27 inch) and cold-formed beams made of thin sheets (d = 0.077 inch and d = 0.049 inch). A range of l/b from 4 to 18 has been covered and center

loading as well as quarter-point loading has been investigated. Strains were measured by means of Huggenberger strain gages and stresses were computed from the strains. Because this test work is part of an extensive research program, sponsored by the American Iron and Steel Institute, the experimental details will be reported elsewhere. The results are summarized in figure 5, which gives the theoretical curves and the experimental results for the eleven beams tested. It is seen that the coincidence of empirical and analytical results is very close throughout the entire range. For this reason it is believed that the equivalent widths computed analytically may safely be recommended for use in design.

## EFFECT OF DISTORTION OF CROSS SECTION

The foregoing analysis is based on the assumption that the flange may be regarded as a plane plate, thus allowing the application of the theory of plane stress. All other authors dealing with this problem have made the same assumption without investigating its validity for wide beams of thin sheet material. Actually, however, the flange is not only curved longitudinally in the loaded beam, but, under the action of the longitudinal bending stresses, also tends to curve in the direction perpendicular to the axis of the beam. For this reason it is necessary to investigate whether or not this double curvature materially affects the stress distribution.

An exact solution of this question would require a mathematical apparatus inappropriately involved for the given purpose. For this reason an approximate method will be used sufficiently exact for the present purpose.

Figure 6(a) represents a part of an I-beam in pure bending; figure 6(b) gives a short element ab of the bottom flange. It is seen that, because of the curvature of the loaded beam, the tensile forces H per unit width of the flange act at an angle $d\varphi$ and hence have a resultant R bisecting this angle, that is, acting in a radial direction. Because H is distributed over the entire width of the flange, R is similarly distributed. Therefore this resultant R acts as a force perpendicular to the surface of the flange tending to bend the flange inward toward the neutral axis. For this reason the distance from the flange surface to the neutral axis

becomes smaller at the outer than at the inner portions of the flange. Because the bending stresses are proportional to this distance to a degree of accuracy sufficient for the present purpose, they decrease from the web toward the edges.

From figure 6(b) it is seen that, per unit length of flange,

$$R = H \frac{d\varphi}{ds} = \frac{H}{r} = \frac{\sigma_x d}{r} \tag{14}$$

where $r$ is the radius of curvature of the bent beam. As shown in figure 6(c), this $R$ represents a transverse load tending to bend the flange. The differential equation for the bending of a long rectangular plate (from reference 5, equation (67)) is:

$$\frac{d^2w}{dy^2} = -\frac{1}{r} = -\frac{M}{D} \tag{15}$$

where $w$ is the deflection of flange

$D$ the flexural rigidity of plate $\left( \frac{E d^3}{12(1 - \nu^2)} \right)$

and $d$ the thickness of plate

It is seen that equation (15) is of the same type as the differential equation for the bending of beams

$$\frac{d^2w}{dy^2} = -\frac{M}{EI}$$

except that the beam rigidity $EI$ is replaced by the plate rigidity $D$. For an exact solution the differential equation

$$d^4w/dy^4 = p/D$$

for cylindrical shells should be used, where $p$ is the total transverse force and consists of $R$ and of the elastic reaction. It can be shown that for the present purpose the numerical difference between the results based upon this exact approach and those obtained by using

equation (15) are negligible. Hence the familiar formulas for the deflections of beams can be applied to those of the flange if $EI$ is replaced by $D$. On this basis the maximum deflection $w_{max}$ (see fig. 6(c)) of the flange out of its plane will now be determined.

It is assumed that $\sigma_x$ and thereby $R$ can be taken as constant throughout the width of the flange which is sufficiently exact for small values of $w$. Then for I-beams from the ordinary cantilever formula (see reference 6, p. 356)

$$w_{max} = \frac{R\, b^4}{8\, D} \tag{16}$$

For an investigation of the stress distribution under actual working conditions, let $\sigma_w$ be the working stress. Then the radius of curvature $r$ of the beam is determined from

$$r = \frac{EI}{M} \quad \text{with} \quad M = \frac{2\, \sigma_w\, I}{h}$$

to

$$r = \frac{E\, h}{2\, \sigma_w} \tag{17}$$

where $I$ is the moment of inertia of the beam. If equation (17) is substituted in equation (14)

$$R = 2\, \sigma_w{}^2\, \frac{d}{E\, h}$$

And from equation (16)

$$w_{max} = 2\, \sigma_w{}^2\, \frac{b^4\, d}{8\, D\, E\, h} = 3 \left(\frac{\sigma_w}{E}\right)^2 \frac{b^4}{d^2 h}\, (1 - \nu^2) \tag{18}$$

The value of $w_{max}$ having been determined, it follows from the linear variation of $\sigma_x$ over the depth of the cross section that the ratio of the maximum stress at $y = 0$ to the minimum stress at $y = \pm b$ is

$$\frac{\sigma_{max}}{\sigma_{min}} = \frac{h}{h - 2\, w_{max}} \tag{19}$$

If the same considerations are applied to box and U-beams and if the generally weak restraint of the flange at the web is neglected, the flange may be regarded in this case as a simple plate freely supported at the webs. From reference 6, p. 360,

$$w_{max} = \frac{5}{384} \frac{RL^4}{D} \tag{20a}$$

or, since here the span $L = 2b$,

$$w_{max} = \frac{5}{24} \frac{Rb^4}{D} \tag{20b}$$

and using again equations (15), (16), (17)

$$w_{max} = 5 \left( \frac{\sigma_w}{E} \right)^2 \frac{b^4}{d^2 h} (1 - \nu^2) \tag{21}$$

If this $w_{max}$ is introduced in equation (19), the stress decrease due to the distortion of the cross section can again be determined.

It is thus seen that the curvature of the beam results in itself in a nonuniform stress distribution in the flanges, which is an effect entirely different from that investigated before on the basis of the distribution of the shearing forces. An exact investigation should therefore consider the joint action of both these effects. It can be shown, however, that in beams of practically possible dimensions the effect of the curvature of the beam is exceedingly small and may therefore be neglected in practical applications.

In order to establish a criterion indicating in which case the effect of the curvature of the beam may be neglected, it will be assumed that a stress decrease of 4 percent is negligible for all practical purposes. Such a stress decrease results in a reduction of the equivalent width of less than 2 percent, which is less than any attainable design accuracy. It is therefore necessary to establish a criterion such that

$$\sigma_{max} - \sigma_{min} \leq 0.04 \sigma_{max} \tag{22}$$

Because the stresses are proportional to the distances from the neutral axis, if equation (18) is used for I-beams

$$\frac{w_{max}}{h/2} = 6\left(\frac{\sigma_w}{E}\right)\left(\frac{b^2}{dh}\right)^2(1 - \nu^2) \leqq 0.04$$

or

$$\frac{b^2}{dh} \leqq \frac{0.0817\ E}{\sqrt{1 - \nu^2}\ \sigma_w} \tag{23a}$$

and, in particular, for steel beams with $E = 3 \times 10^7$ pounds per square inch

$$\frac{b^2}{dh} \leqq \frac{2.57 \times 10^6}{\sigma_w} \tag{23b}$$

where b, h, d are, respectively, half the flange width, the depth, and the flange thickness of the beam; $\sigma_w$, the working stress; and $\nu$, Poisson's ratio.

Similarly for box beams, if equation (21) is used

$$\frac{w_{max}}{h/2} = 10\left(\frac{\sigma_w}{E}\right)^2\left(\frac{b^2}{dh}\right)^2(1 - \nu^2) \leqq 0.04$$

or

$$\frac{b^2}{dh} \leqq \frac{0.0633\ E}{\sqrt{1 - \nu^2}\ \sigma_w} \tag{24a}$$

and particularly for steel beams

$$\frac{b^2}{dh} \leqq \frac{1.98 \times 10^6}{\sigma_w} \tag{24b}$$

employing the same symbols as above.

Hence, the data for the equivalent width given in table I and figure 4 may be applied to any beam satisfying the conditions expressed in equations (23) and (24).

It may easily be verified numerically that practically all beams with structurally possible dimensions will satisfy these conditions.

## CONVERGENCE OF THE SERIES INVOLVED

In the foregoing analysis, the reduction factor $2b'/2b$ as well as the stress concentration $\sigma_{max}/\sigma_{min}$ are obtained as quotients, the numerator and the denominator of which are in the form of a Fourier series. The numerical values given in tables I and II have been obtained by taking nine terms of each of the series involved. In order to obtain an estimate of the accuracy thus obtained, it seems advisable to analyze the question of the convergence of these series. This analysis will be made here for I-beams only because the method is essentially the same for box beams.

In order to investigate the numerator of equation (13a), the coefficients $A_n$, $B_n$, $C_n$, $D_n$ from equations (9) are substituted in equation (6), which results in

$$\left.\frac{\partial \phi}{\partial y}\right|_{y=0}^{y=b} = \sum_{1}^{n} \frac{K_n}{\alpha_n}$$

Substitution of the appropriate $K_n$ from equations (11) gives for uniformly distributed load

$$\sum_{1}^{n} \frac{K_n}{\alpha_n} = \sum_{1}^{n} \pm \frac{1}{n^2} \frac{2l}{n\pi} = \sum_{1}^{n} \pm \frac{\text{const}}{n^3}$$

and for concentrated load

$$\sum_{1}^{n} \frac{K_n}{\alpha_n} = \sum_{1}^{n} \frac{1}{n} \frac{2l}{n\pi} = \sum_{1}^{n} \frac{\text{const}}{n^2}$$

It is seen that each of these expressions is an absolutely convergent series, the first few terms of which decrease rather rapidly.

Making the same substitutions in the denominator of equation (13a), one arrives at

$$\left(\frac{\partial^2 \phi}{\partial y^2}\right)_{y=o} = \sum_1^n (A_n \alpha_n^2 + 2 D_n \alpha_n)$$

$$= - \sum_1^n K_n \frac{(3 + \nu) \cosh^2 \alpha_n b + (1 - \nu) + (1 + \nu)(\alpha_n b_n)^2}{2 \sinh \alpha_n b \cosh \alpha_n b + 2 \alpha_n b}$$

Because the hyperbolic functions involved increase exponentially with $\alpha_n$, it is seen that for higher terms ($\alpha_n$ large) the individual terms of this series approach the corresponding terms of

$$\sum_1^n K_n \frac{3 + \nu}{2} \coth \alpha_n b \cong \frac{3 + \nu}{2} \sum_1^n K_n$$

because for large $\alpha_n$ $\coth \alpha_n b \cong 1$. If for uniformly distributed load $K_n$ is substituted from equation (11a), it is seen that the higher terms of this series are of the type $\sum_1^n \pm \frac{\text{const}}{n^2}$, which again is absolutely convergent. For concentrated load, however, substitution of $K_n$ from equation (11b) gives a series the higher terms of which are seen to approach those of the series $\sum_1^n \frac{\text{const}}{n}$ while the first few terms of the former series decrease more rapidly than those of the latter. Hence, the series for the denominator of equation (13a) for concentrated load is divergent, although the individual terms approach zero with increasing n and the first few terms decrease rather rapidly.

In a purely mathematical sense this divergence does not threaten the validity of the solution. Indeed, $\phi$ (equation (6)) satisfies the original differential equation (4) not only as a series but term by term. Hence, the series may be broken off at any arbitrary term and the sum will still satisfy equation (4) and all other equations derived from it. Therefore, the problem consists in the physical rather than in the mathematical legitimacy of taking a small number of terms of a divergent series.

It will be remembered that by means of the first of the four boundary conditions the given shear distribution

at $y = 0$ is expressed in a Fourier series, the coefficients of which are $K_n$. In order to obtain full coincidence of this series with the shear diagram of figure 3(b), one would have to take an infinite number of terms. Breaking the series off after nine terms means that the discontinuous curve of figure 3(b) is replaced by a continuous, though sharply changing, curve. As an example such a curve, but for four terms, is given in figure 7(a) (reference 7, p. 63). For nine terms, part a of this curve will be correspondingly shorter. If one now regards the closely corresponding curve of figure 7(b) as the diagram of shear distribution it is seen that it corresponds to a loading of the kind of figure 7(c) rather than to an ideally concentrated load. The length a is equal to one-half the wave length of the last sine wave added, i.e., to span/n or in our case to span/17. However, the actual shear distribution will just be of this same kind for the following two reasons: All concentrated loads actually are distributed over a small length c (fig. 7(c)) of the span and, before reaching the web, the resulting shear will be further distributed in the web. Therefore, by taking a definite number of terms, the analysis is based on a shear distribution which, in essence, is exactly of the kind actually occurring under concentrated loads.

It remains to verify whether taking nine terms of the corresponding series is sufficiently accurate for the given purpose. This question may be answered in the affirmative for the following three reasons:

1) In actual structures concentrated loads usually are distributed over a length along the span of not less than span/50. Without detailed investigation of this question, it may safely be assumed that the further distribution in the web doubles or even triples this length.

2) The reduction factor $2b'/2b$ changes very little with decreasing values of a. For instance, for a beam of $l/b = 2\pi$, $2b'/2b = 0.828$ for six terms and $2b'/2b = 0.791$ for nine terms. Thus an increase in the length a of about 55 percent (span/11 instead of span/17) results in an increase of less than 5 percent in the equivalent width. For higher terms this difference becomes still smaller.

3) The experimental results summarized in figure 5 have been obtained by applying loads in some cases directly through rollers and, in other cases, through distributing plates of width = span/24 to span/48. The good coincidence of analytical and empirical results is sufficient proof for the adequacy of the chosen number of terms.

## GENERAL CONCLUSION

The primary purpose of the investigation was to analyze the stress distribution in the flanges of wide, thin-wall beams of I, T-, U-, and box shape and to obtain results suitable for direct application in design. It is shown that the magnitude of the bending stresses in the flanges of such beams varies across the width of the section and that the amount of this variation depends upon the dimensions of the beam and upon the type of loading.

Therefore, in the determination of the magnitude of the maximum bending stress in design work, the equivalent width of such flanges should be used instead of the actual width. In figure 4 curves are given from which this equivalent width can be read directly for any particular type of beam and loading.

For the purpose of facilitating the experimental verification of the analytical results, further curves have been computed that give the ratios of the maximum to the minimum bending stress in the flanges. These ratios have been checked experimentally by means of strain measurements on 11 I-beams. The experimental data confirm very satisfactorily the analytical results.

It is further shown that the cross sections of wide beams made of extremely thin sheets are subject to distortion that gives rise to additional stress concentration. Equations (23) and (24) furnish simple conditions for determining the limiting dimensions of beams for which the effect of this distortion may be neglected in practical applications. It may easily be verified numerically that practically all beams of structurally possible dimensions will satisfy these conditions.

College of Engineering, School of Civil Engineering,
Cornell University, Ithaca, N. Y., June 1940.

## REFERENCES

1. von Kármán, Th.: Die mittragende Breite (The Effective Width), pp. 114-127 of Beiträge zur technischen Mechanik und technischen Physik (Contributions to Technical Mechanics and Technical Physics). (Festschrift, August Föppl). Julius Springer (Berlin) 1924.

2. Schnadel, G.: Die mittragende Breite in Kastenträgern und im Doppelboden. Werft Reederei Hafen, no. 5, March 7, 1928, pp. 92-101.

3. Chwalla, E.: Formulas for the Determination of Effective Width of Thin Flange and Rib Plates. Der Stahlbau, vol. 9, no. 17, May 8, 1936, pp. 73-78.

4. Timoshenko, S.: Theory of Elasticity. McGraw-Hill Book Co., Inc., 1st ed., 1934, p. 25.

5. Timoshenko, S.: Strength of Materials. Vol. II. D. Van Nostrand Co., Inc., 1930, p. 476.

6. Anon.: Steel Construction; a Manual for Architects, Engineers and Fabricators of Buildings and Other Steel Structures. Amer. Inst. of Steel Const., 1939.

7. Byerly, W. E.: An Elementary Treatise on Fourier's Series and Spherical, Cylindrical, and Ellipsoidal Harmonics, with Applications to Problems in Mathematical Physics. Ginn & Co., 1893, p. 63.

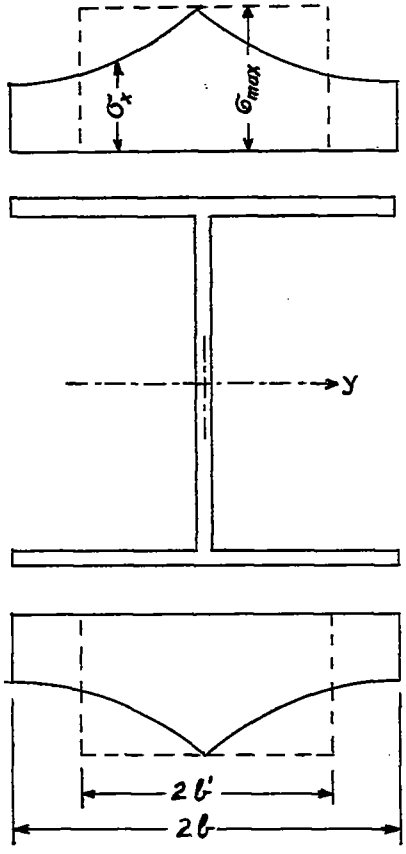


Figure 1.- Actual stress distribution over width of flange of I-beam.

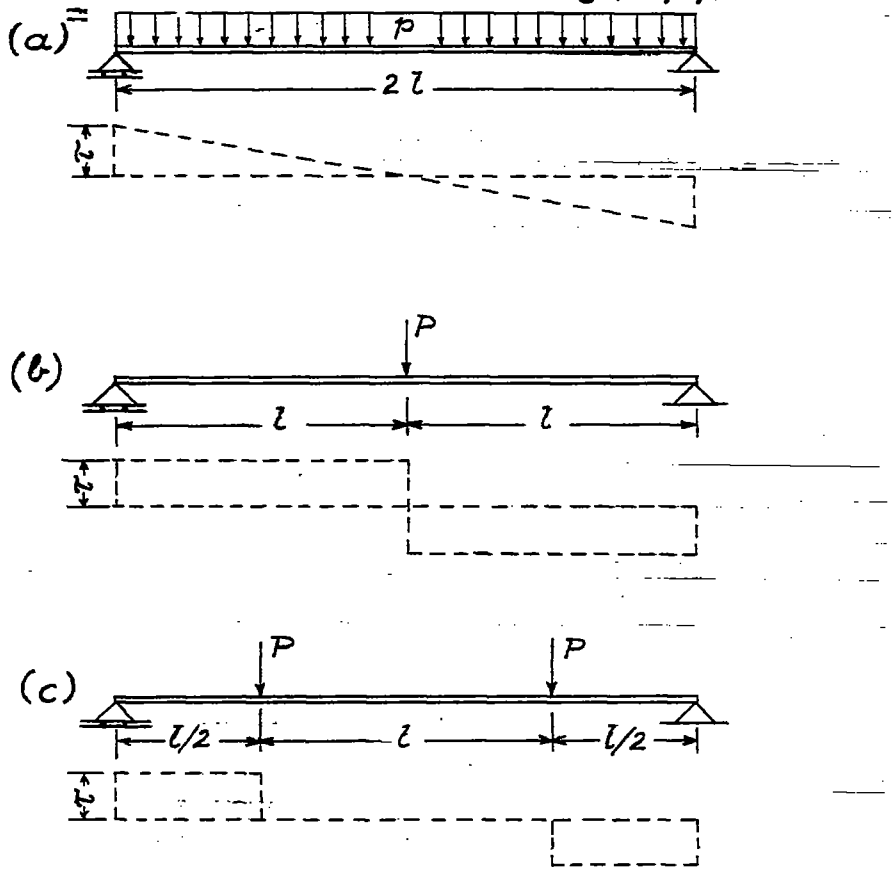


Figure 3.- Shear distribution for the three types of loading analyzed. (a) Uniformly distributed load. (b) Single concentrated load applied in the center. (c) Two concentrated loads of equal magnitude applied at quarter points.

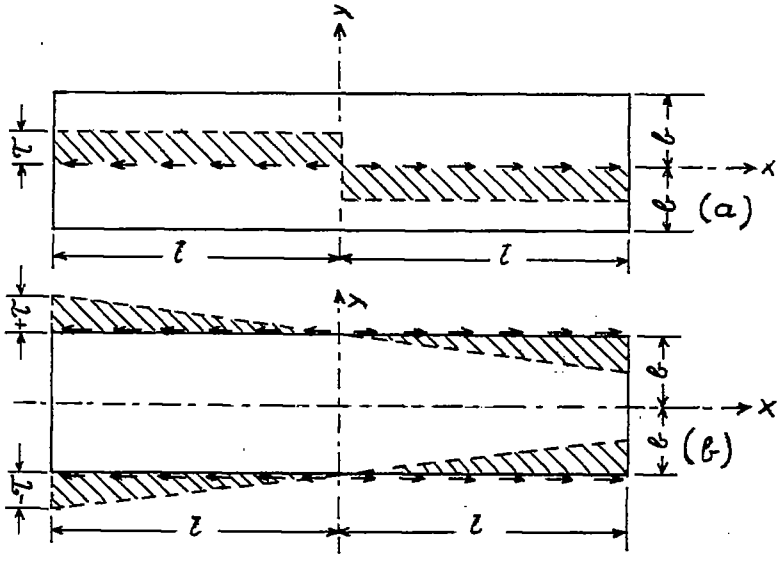


Figure 2.- Distribution of applied shear stress, transmitted from web to flange. (a) Flange of I-beam loaded by a single concentrated force in the center. (b) Flange of box beam under uniform load.

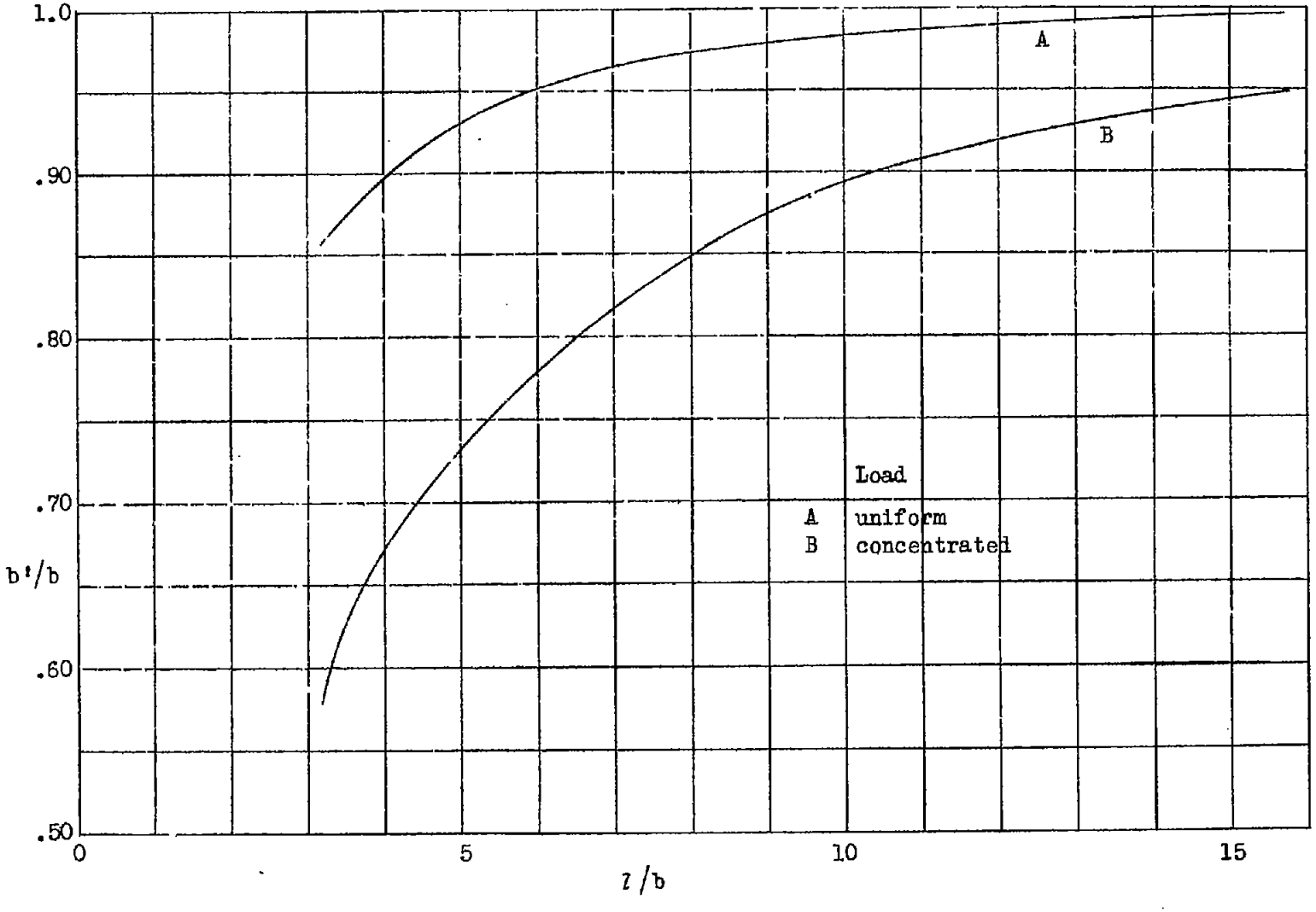


Figure 4.- Analytical curves for determining the equivalent width of the flanges of I-, T-, U-, and box beams. $l/b$ = span/width, $b'/b$ = equivalent width / actual width.

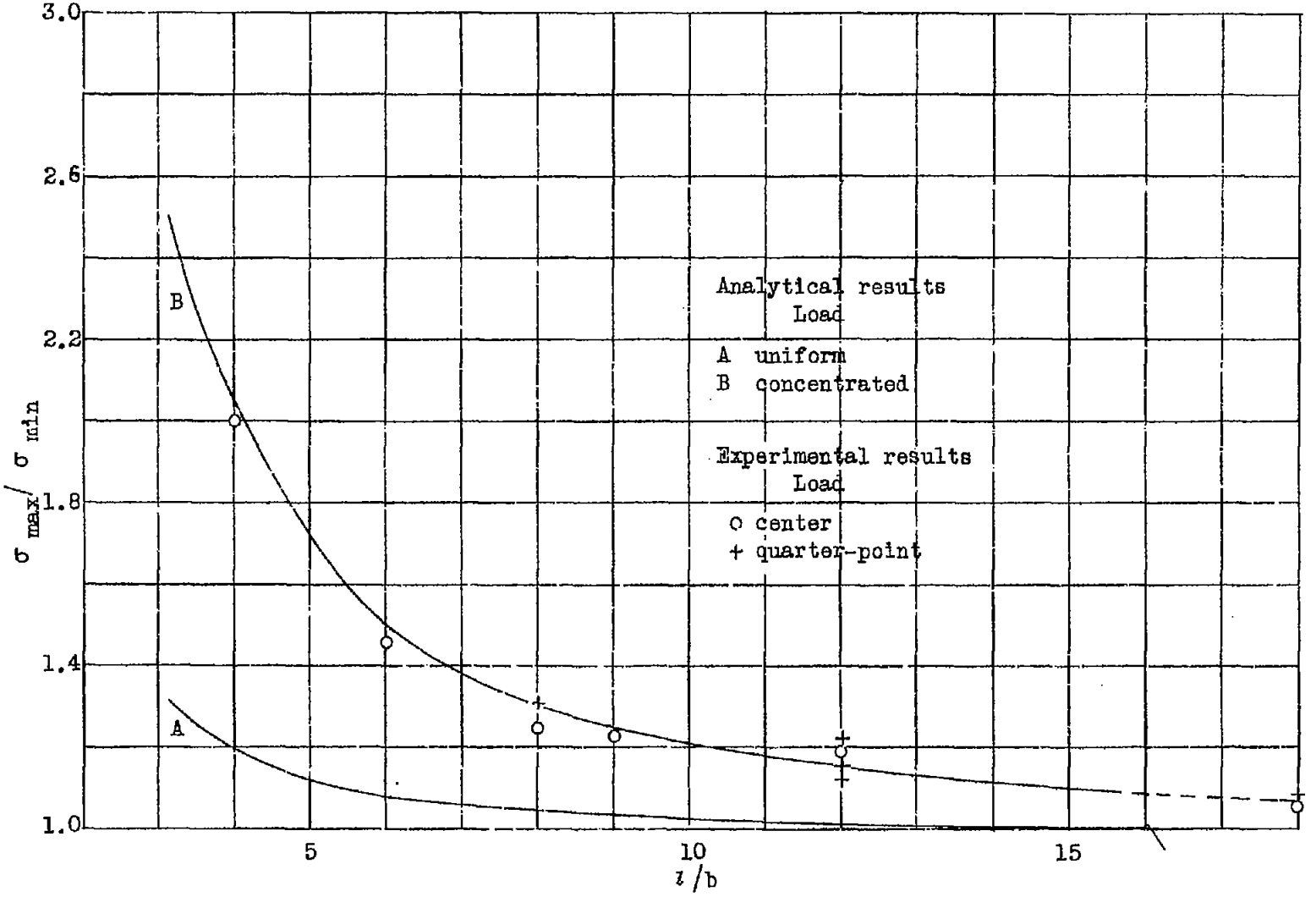


Figure 5.- Analytical stress concentration curves for I- and T-beams and experimental results of 11 I-beams tested. $\sigma_{max}$ = bending stress at joint of web and flange, $\sigma_{min}$ = bending stress at outer edge of flange, l/b = span/width.

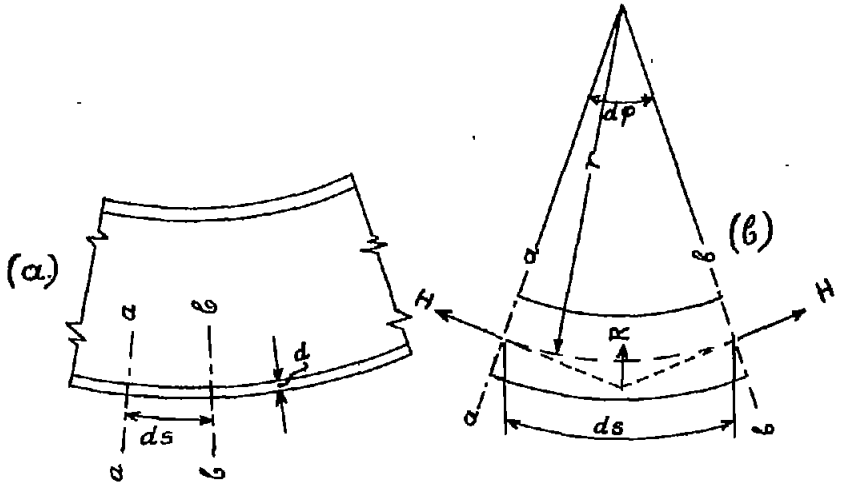


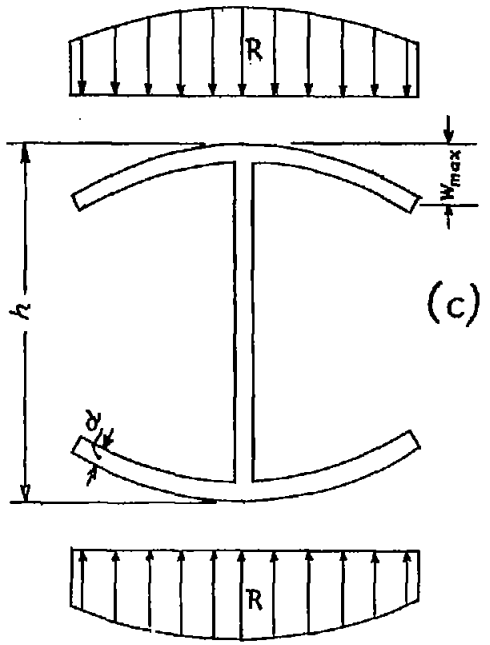


Figure 6.- Actual stress distribution over width of flange due to distortion of cross section of I-beam. (a) Side-view of section of I-beam. (b) Element, ab, of bottom flange. (c) Distorted cross section and stress distribution.

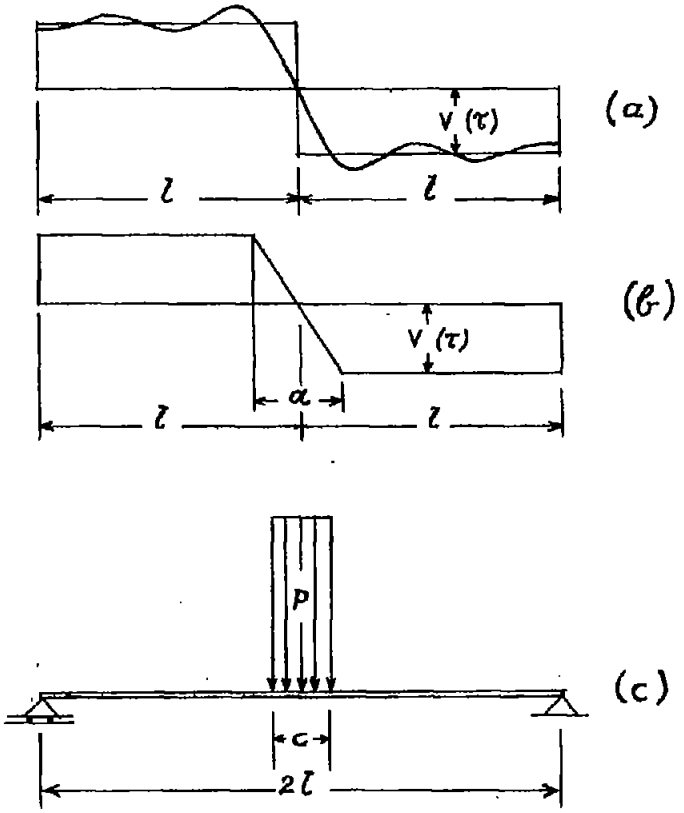


Figure 7.- Shear distribution of beam loaded by concentrated force in center; representation of the actual shear distribution by four terms of a Fourier series.

Figs. 6,7